Infiltration of Fiber Preforms by a Binary Alloy: Part I. Theory

A. MORTENSEN and V. MICHAUD

During infiltration of a fiber preform by a binary hypoeutectic alloy, solid metal can form in the composite because of cooling at the fibers or at the mold wall. Contrary to the case of an unalloyed matrix, temperature, composition, and fraction solid may vary in the composite. This results in macrosegregation and microstructural heterogeneity within the composite casting. It is shown that solid metal that forms because of cooling at the fibers grows gradually behind the infiltration front, while the local temperature increases. Metal superheat, when present, serves to progressively remelt solid metal in the composite during infiltration and increases compositional and microstructural heterogeneity within the composite. General expressions are derived to describe heat, mass, and fluid flow during the infiltration process. In the case of unidirectional adiabatic infiltration driven by a constant applied pressure, a similarity method can be used to reduce the mathematical complexity of the problem. Numerical solution of the resulting equations then allows us to predict temperature, fraction solid, and composition profiles within the composite. With the further assumption of negligible thermal conduction, the problem lends itself to an analytical solution. The analysis is performed for the case of unidirectional adiabatic infiltration under constant applied pressure of 24 vol pct δ-alumina preforms by Al-4.5 wt pct Cu. Results indicate that there is significant latitude for control of macrosegregation and microstructure within cast fiber-reinforced alloys.

I. INTRODUCTION

A fluid flow and heat transfer analysis relevant to the production of metal matrix composites by infiltration of porous preforms with pure liquid metal was recently presented.[1] This analysis incorporated results from previous studies of the process by Nagata and Matsuda,[2,3] Fukunaga,[4] and Fukunaga and Goda[5,6] and agreed with experimental data on the infiltration of δ-alumina fiber preforms by pure aluminum.[7] In brief, theoretical treatment of the process was based on a treatment of the simpler case of unidirectional infiltration. In this configuration, it was shown that fluid flow and heat transfer can be treated by a similarity method provided there is no external cooling and provided the applied pressure is constant, allowing for an analytical solution. Of particular interest was the fact, first identified in References 2 through 6, that if the fiber preform temperature is initially below the metal melting point, solid metal forms at the infiltration front. This phenomenon strongly influences both the rate of infiltration and the microstructure of the composite.

Experiments utilizing the same infiltration process have shown that with a low initial fiber temperature, composites of δ-alumina fibers infiltrated with Al-4.5 wt pct Cu display macrosegregation within the matrix.[8] The source of concentration gradients over the length of the composite is simple to understand: when the fiber temperature is below the metal liquidus, solid metal forms at the infiltration front. This solid metal is mechanically trapped by the fibers and remains where it formed. The flowing liquid is richer in solute than the solid it leaves behind, resulting in solute enrichment downstream of the path followed by the infiltration front. This, in turn, leads to macrosegregation in the matrix of the cast composite. In a study of the infiltration process, Clyne and Mason[9] showed that within an Al-2.5 wt pct Mg matrix alloy, significant grain size variations can be observed after infiltration by squeeze casting into δ-alumina fiber preforms. When the initial fiber preform temperature was below the liquidus temperature, the matrix of the composite exhibited a two-zone structure: fine grains, of a size roughly equal to the interfiber spaces, downstream of the infiltration path and large columnar grains upstream where the metal entered the preform. Only the second zone, featuring large columnar grains, was present when the initial fiber preform temperature was above the alloy liquidus.[9] These observations indicate that variations in matrix microstructure and composition are obtained when the initial fiber temperature is below the matrix liquidus. This condition is prevalent in most casting procedures, usually to minimize chemical interaction between fibers and matrix.

This paper addresses these issues from a theoretical standpoint and follows the order of presentation adopted in the treatment of infiltration by a pure metal.[1] Namely, after a formulation of the general problem, a solution for adiabatic unidirectional infiltration with a hypoeutectic alloy under constant applied pressure is given. Numerical results for Al-4.5 wt pct Cu cast into δ-alumina fiber preforms are then presented as a practical example.

II. THE GENERAL PROBLEM

Consider the infiltration of a fibrous preform by a binary metal alloy of nominal composition C_0. The phase diagram of this alloy is assumed to be of the eutectic

A. MORTENSEN, ALCOA Assistant Professor, and V. MICHAUD, Research Assistant, are with the Department of Materials Science and Engineering, Massachusetts Institute of Technology, Cambridge, MA 02139.

Manuscript submitted August 4, 1989.

type and the alloy to be hypoeutectic; *i.e.*, $C_0 < C_E$, where C_E is the eutectic composition. A fiber preform is placed within a die, into which metal is injected at a pressure sufficiently high for it to form a composite material by penetrating the space between the fibers. In general, the initial fiber temperature T_f, the initial mold temperature T_i, and the initial metal temperature T_0 are all different. The metal, fibers, and mold, therefore, exchange heat during the process.

As in the problem of infiltration by a pure metal matrix, cooling of the metal by the preform and/or the mold results in metal solidification between the fibers while flow of the liquid metal is taking place. Several regions can then coexist within the preform during infiltration, depending on processing parameters, such as T_f, T_i, and T_0.

As with a pure metal, the number and nature of these regions depend on casting conditions. With an initial fiber preform temperature T_f higher than the alloy liquidus, liquid metal will enter the preform but will only solidify due to cooling from the mold walls. The problem is then one of alloy solidification concomitant with intense fluid flow, in many respects similar to problems treated in casting fluidity.[10] Conversely, a low initial fiber temperature will result in intense cooling of the metal as it encounters the cold fibers at the infiltration front. This will result in the formation of solid metal in the vicinity of the infiltration front, which serves to raise the local temperature by release of latent heat. Local temperature may also increase because of heating by incoming metal or may decrease because of cooling at the mold walls. Thus, a region in the casting will form where solid and liquid metal coexist because of cooling by the fibers and cooling at the mold wall (region 1 in Figure 1). A fully

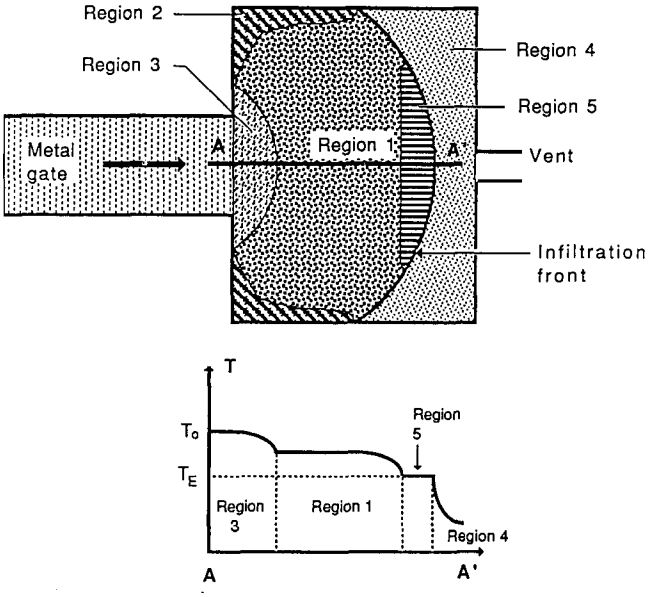

Fig. 1—Schematic illustration of the injection of an alloy into a mold containing a fiber preform under conditions such that eutectic solid metal forms at the infiltration front. The fiber preform then contains five regions, as shown in the figure: region 1 where primary solid and liquid metal coexist, region 2 where the matrix is solid due to external cooling, region 3 where the matrix is liquid due to heating by incoming metal, region 4 where the matrix has not reached the fibers, and region 5 where solid and liquid eutectic metal coexist.

solid region may appear along the mold walls because of heat exchange between mold and casting (region 2). At the preform entrance, superheated metal entering the casting will remelt solid metal present in region 1 or 2, creating a region where only liquid metal coexists with the fibers (region 3). Region 4 is the uninfiltrated part of the preform, from which gas is expelled through a vent. Provided the initial fiber preform temperature is sufficiently low, an additional region where the solid phase is of eutectic composition may form in the vicinity of the infiltration front. We define this region as region 5, as opposed to region 1, where the solid metal is the primary phase of the eutectic alloy.

The driving force for flow of metal can be provided by capillary forces for a wetting system; otherwise, an external application of pressure on the metal at the preform entrance is necessary. This applied pressure determines, together with the amount, location, and morphology of solid metal in regions 1, 2, and/or 5, the rate of infiltration.

As with a pure matrix, solid metal in region 1 is assumed to remain where it formed, because it is trapped by the fibers. With an alloy, however, the problem is complicated by the addition of mass transport to fluid flow and heat transfer present in the former case. A further complication arises from the fact that solidification can take place over a range of temperatures so that significant gradients in temperature, concentration, and fraction solid metal can exist within region 1. The presence of solute in the matrix thus adds two variables within region 1, namely, composition and fraction solid metal, which must be calculated together with flow rate and local temperature.

A mathematical formulation of the problem together with an analysis of the novel solidification problem present when the initial fiber temperature is low enough to cause metal solidification during infiltration are presented in Section III.

III. ASSUMPTIONS AND GENERAL EQUATIONS

A. *Fluid Flow*

As in Reference 1, we treat infiltration by considering a volume element ΔV large enough to represent significant average values of local composite characteristics but small enough to be treated as a differential element within the composite. Within ΔV, the fibers occupy a local volume fraction V_f and the metal, a volume fraction V_m of which a volume fraction g_s is solid. We assume that the metal and the preform are incompressible and ignore density differences between the solid and liquid metal. The coordinate system is fixed with respect to the fiber preform.

As in Reference 1, we simplify capillary phenomena and assume that the infiltration front is sharp. The expression $1 - V_f$ then equals V_m everywhere in the infiltrated composite, comprising regions 1 through 3 and 5 in Figure 1. The pressure in the composite at the infiltration front is $P_g + \Delta P_\gamma$, where ΔP_γ is the capillary pressure drop at the infiltration front and P_g is pressure in the gas within region 4. The value of $\Delta P_\gamma > 0$

corresponds to nonwetting, while $\Delta P_\gamma < 0$ corresponds to wetting of the fibers by the metal. We assume that ΔP_γ is independent of the infiltration front velocity.

We assume that flow of liquid metal through ΔV, measured by the superficial velocity $\mathbf{v}_o$, is within the range of validity of Darcy's law:

$$\mathbf{v}_o = -\frac{\mathbf{K}}{\mu}(\nabla P - \rho_m g) \quad [1]$$

where μ is the viscosity of the liquid metal, $\mathbf{K}$ is the symmetric permeability tensor of the preform, P is the average pressure in the volume element, ρ_m is the metal density, and g is the acceleration due to gravity.

The continuity equation is

$$\nabla \mathbf{v}_o = 0 \quad [2]$$

Equations [1] and [2] are valid in regions 1, 3, and 5 of the composite. For a fiber preform of uniform volume fraction V_f, fiber distribution, and fiber diameter, the permeability $\mathbf{K}$ in ΔV is only a function of the local volume fraction and morphology of the solid metal. The viscosity, μ, is a function of temperature and composition. The range of validity of Darcy's law for flow of a metal through a fibrous preform is discussed in Appendix I of Reference 1.

B. *Heat Transfer*

We assume that the fiber diameter is sufficiently small so that the temperature T is uniform within ΔV. As with the pure metal, we neglect viscous heat dissipation. The validity of these assumptions is examined in Appendix I of Reference 1.

We assume that the interface between solid and liquid metal is everywhere at equilibrium, and we neglect the effect of curvature on the matrix alloy phase diagram. Because the matrix is an alloy, heat transfer is possible within region 1. The heat transfer equation within that region of the composite must include a term for variation in volume fraction solid metal, in addition to terms accounting for heat transfer by conduction and convection into ΔV, which were included in Eq. [3] of Reference 1. The heat transfer equation is thus

$$\nabla \cdot (\mathbf{k}_c \nabla T) = \rho_c c_c \frac{\partial T}{\partial t} + \rho_m c_m \mathbf{v}_o \cdot \nabla T - \rho_m \Delta H (1 - V_f) \frac{\partial g_s}{\partial t} \quad [3]$$

within region 1, where $\mathbf{k}_c$ is the thermal conductivity tensor of the composite, ΔH is the latent heat of solidification of the alloy, g_s is the fraction solid metal, ρ is density, c is heat capacity, and the subscripts m, f, and c refer to the metal, fiber, and composite, respectively.

Within region 2, all metal is solid and there is no flow. We, therefore, apply Fourier's law:

$$\nabla \cdot (\mathbf{k}_c \nabla T) = \rho_c c_c \frac{\partial T}{\partial t} \quad [4]$$

Within region 3, there is no solid metal and the heat transfer equation is the same as Eq. [3] of Reference 1:

$$\nabla \cdot (\mathbf{k}_c \nabla T) = \rho_c c_c \frac{\partial T}{\partial t} + \rho_m c_m \mathbf{v}_o \cdot \nabla T \quad [5]$$

Within region 4, the uninfiltrated preform, we neglect the contribution to heat transfer of the gas phase and use Fourier's law:

$$\nabla \cdot (\mathbf{k}_p \nabla T) = \rho_p c_p \frac{\partial T}{\partial t} \quad [6]$$

where the subscript p designates characteristics of the preform. Since the heat capacity of the gas phase initially surrounding the fibers is likely to be negligible, $\rho_p c_p$ is generally equal to $V_f \rho_f c_f$.

In region 5, liquid and solid eutectic metal coexist. From our assumption of local equilibrium at the solid/liquid interface, there is no heat transfer within this region which is uniformly at the eutectic temperature T_E:

$$T = T_E \quad [7]$$

C. *Solidification*

With a pure metal, we assumed that the solid metal grew in the shape of a uniform layer coating the fibers. The justification for this assumption is that solidification of a pure metal is governed by heat evacuation from the solidification front. The growing solid phase is then expected to be attracted by the cold fibers, since they represent a heat sink for the growing solid metal. In the case of an alloy, solidification is also governed by solute diffusion in the liquid away from the solidification front. Whereas the fibers act as sinks with regard to enthalpy evacuation, they represent barriers to solute diffusion. The solidification mechanism is, therefore, different in the case of an alloy, and the assumption that the solid phase forms a uniform coating surrounding the fibers is no longer reasonable. Experimental confirmation of this assertion is given in Reference 11, where infiltration rates with 99.9 pct pure aluminum were shown to differ from those with 99.999 pct pure aluminum under identical conditions. These data are most plausibly explained by a change in solidification morphology of the metal with the addition of 0.1 pct impurities. Studies of solidification of Al-4.5 wt pct Cu, furthermore, have shown that growth of the primary phase takes place within the interfiber spaces in avoidance of the fibers when the fibers and metal are cooled simultaneously and are, therefore, at similar temperatures.[12] We, therefore, expect the relationship between volume fraction solid metal and permeability $\mathbf{K}$ of the porous medium consisting of solid metal and fibers to be more complex than that with a pure metal. For this reason, we assume here that a functional relationship exists between volume fraction solid metal g_s and permeability $\mathbf{K}$ but do not specify its nature. We consider the infiltration velocity to be a parameter and do not treat its correlation with applied pressure.

It will be shown in Section III–E–3 that solidification of the metal induced by cooling at initially cold fibers cannot take place at the infiltration front, as with pure metal. Instead, the solid alloy metal grows gradually, behind the infiltration front. While solidification is taking place, the local temperature can either decrease

(because of cooling from the mold walls) or increase (because of heating by incoming metal). The direction in which temperature varies influences microsegregation in the solid metal phase.

Local equilibrium dictates that the solid be of the local solidus composition. If local temperature is decreasing, solid metal formed earlier is thermodynamically stable and will either retain its composition or increase its solute content by solid-state diffusion, a process that has been shown to be very significant in metal matrix composites at low cooling rates.[12] On the other hand, immediately behind the infiltration front, where temperature is increasing, any solid formed earlier is thermodynamically unstable (unless the solidus is retrograde, which we assume here not to be the case). Solidification must, therefore, follow the equilibrium lever rule when local temperature is increasing. Since local temperature will first increase behind the infiltration front and subsequently decrease due to cooling from the mold wall, we expect solute concentration profiles in the final solid metal of the cast composite to feature a core of low solute content within the primary phase.

D. *Mass Transport*

We make the assumption, conventional in solidification theory,[13] that the liquid phase between dendrites and/or fibers within ΔV is uniform in composition. Because flow of the liquid metal is vigorous in infiltration of metal matrix composites, we assume that solute enters or leaves ΔV only by convection and neglect mass flow by diffusion in or out of ΔV. The validity of this assumption can be estimated by referring to Figure 4 of Reference 1 for the particular infiltration rate and diffusion coefficient of interest.

Mass transport is, therefore, governed within region 1 by conservation of mass in the volume element ΔV:[14]

$$\frac{\partial \bar{C}}{\partial t} = -\nabla\{(1 - g_s)\, C_L \cdot \mathbf{v}\} \qquad [8]$$

where $\bar{C}$ is the local average matrix composition in ΔV, C_L is the composition of the liquid, and $\mathbf{v}$ is the local velocity of interdendritic liquid relative to solid. The local velocity $\mathbf{v}$ is related to the superficial velocity $\mathbf{v_o}$ by

$$\mathbf{v} = \frac{\mathbf{v_o}}{(1 - V_f)\,(1 - g_s)} \qquad [9]$$

Combining Eqs. [8], [9], and [2], the solute conservation equation takes the form

$$\frac{\partial \bar{C}}{\partial t} = -\frac{\mathbf{v_o}}{1 - V_f} \cdot \nabla C_L \qquad [10]$$

In region 3, as long as the metal has had no previous exposure to solid metal, its composition is everywhere C_0, the nominal composition. In region 5, the metal is uniformly at the eutectic composition, C_E.

E. *Interregion Boundary Conditions*

Conservation and continuity equations can be derived for each of the boundaries separating regions 1 through 5 which, together with governing equations within each of the regions, allow modeling of a given infiltration process for a chosen set of initial parameters.

1. *Boundary 1-2*

With sluggish solid-state diffusion or matrix composition above the maximum solid solubility limit, this boundary will correspond to solidification of the last pool of liquid metal at the eutectic temperature. In this case, the equations are

$$T_1 = T_2 = T_E \qquad [11a]$$

$$(\mathbf{k}_c \nabla T_2) \cdot \mathbf{n}_{1,2} = (1 - V_f)\,(1 - g_{s1})\,\Delta H \rho_m v_{1,2} \qquad [12a]$$

$$\mathbf{v_{o1}} \cdot \mathbf{n}_{1,2} = 0 \qquad [13]$$

In these and following equations, the subscript i signifies within region i along the boundary, $\mathbf{n}_{i,j}$ is the normal to the boundary separating regions i and j, oriented from i to j, $v_{i,j}$ is the local boundary velocity oriented from i to j and $\mathbf{v}_{i,j} = v_{i,j}\mathbf{n}_{i,j}$.

If the eutectic temperature is not attained when external cooling at the mold wall fully solidifies the matrix, solidification must be gradual, and the fraction solid is $g_s = 1$ in region 1 with no discontinuity at the boundary. This is because an abrupt change in g_s across the boundary above the eutectic temperature would necessitate evacuation of solute into region 1, which cannot take place by convection (Eq. [13]). We, therefore, have, in this case,

$$T_1 = T_2 \qquad [11b]$$

$$(\mathbf{k}_c \nabla T_2) \cdot \mathbf{n}_{1,2} = (\mathbf{k}_c \nabla T_1) \cdot \mathbf{n}_{1,2} \qquad [12b]$$

$$\mathbf{v_{o1}} \cdot \mathbf{n}_{1,2} = 0 \qquad [13]$$

2. *Boundary 1-3*

Here, melting of solid metal in region 1 is taking place due to heating from the liquid metal flowing in from the gate. Since it is not likely that the metal would have experienced a local decrease in temperature prior to remelting, we assume that solidification is according to the equilibrium lever rule. Because we assume no solute diffusion over distances on the scale of the casting dimensions, the remelting front is sharp, with a decrease in liquid composition from regions 3 to 1 due to the remelting of solute-poor solid.

$$P_1 = P_3 \qquad [14]$$

$$T_1 = T_3 \qquad [15]$$

$$C_{L3} = C_0 \qquad [16]$$

$$(C_0 - C_{L1})\mathbf{v_{o1}} \cdot \mathbf{n}_{1,3} = (C_0 - (1 - (1 - k)g_s)C_{L1})v_{1,3} \qquad [17]$$

$$-(\mathbf{k}_c(\nabla T_3 - \nabla T_1)) \cdot \mathbf{n}_{1,3} = (1 - V_f) g_s\, \Delta H\, \rho_m v_{1,3} \qquad [18]$$

$$(\mathbf{v_{o1}} - \mathbf{v_{o3}}) \cdot \mathbf{n}_{1,3} = 0 \qquad [19]$$

3. *Boundary 1-4*

This is the infiltration front when the fibers are sufficiently cold to cause solidification of the infiltrating matrix. It can be shown that the fraction solid metal at the infiltration front, *i.e.*, in region 1 at this boundary, is zero. Suppose there is a finite fraction solid metal g_s at the front and liquid of composition C_L, at time t and

position x. At time $t + dt$, the infiltration front reaches position $x + dx$, where liquid formerly at x and of composition C_L meets new fibers and solidifies a fraction $g_s + dg_s$ to generate a finite fraction solid at the tip. Therefore, since formation of a finite amount of solid is accompanied by rejection of a finite amount of solute, the composition in the liquid must, in turn, increase by a finite amount. This results in a discontinuity of C_L between x and $x + dx$, which is impossible because this implies an infinite temperature gradient (from local equilibrium) in violation of our assumption of a finite thermal diffusivity in the composite.

The equations are, therefore,

$$P_1 = P_g + \Delta P_\gamma \quad [20]$$

$$T_1 = T_4 \quad [21]$$

$$g_s = 0 \quad [22]$$

$$(\mathbf{k}_p \nabla T_4) \cdot \mathbf{n}_{1,4} = (\mathbf{k}_c \nabla T_1) \cdot \mathbf{n}_{1,4} \quad [23]$$

$$\mathbf{v}_{o1} = (1 - V_f)\mathbf{v}_{1,4} \quad [24]$$

4. *Boundary 1-5*

If the fibers are still colder, the first solid metal to form may be of the eutectic composition. This metal will solidify at the infiltration front itself, like a pure metal and unlike the primary phase, because there is no global solute rejection by the solid. Where temperature starts to rise above the eutectic temperature due to liquid entering the preform, the eutectic remelts and new (primary) solid metal grows. As with the boundary between regions 1 and 4, the fraction solid primary metal must be zero in region 1 at the boundary between regions 1 and 5. For a proof, suppose there is a finite fraction primary solid metal g_{s1} in region 1 at the boundary between regions 1 and 5, with liquid of composition C_E, at time t and position x. At time $t + dt$, the boundary reaches position $x + dx$, where solid of composition C_E remelts and solidifies a fraction $g_{s1} + dg_{s1}$ to ensure a finite fraction solid in region 1 at the boundary. The composition in the liquid at this point, therefore, has to increase by a finite amount due to solute rejection by the solid. This results in a discontinuity in C_L at x and at $x + dx$. This is impossible because it implies an infinite temperature gradient (from local equilibrium), which violates our assumption of finite thermal diffusivity in the composite. The equations are, therefore,

$$P_1 = P_5 \quad [25]$$

$$T_1 = T_5 = T_E \quad [26]$$

$$-(\mathbf{k}_c \nabla T_1) \cdot \mathbf{n}_{1,5} = (1 - V_f) g_{sE} \Delta H \rho_m v_{1,5} \quad [27]$$

$$C_1 = C_5 = C_E \Rightarrow g_{s1} = 0 \quad [28]$$

5. *Boundary 2-3*

Such a boundary would represent a sharp "planar" solidification front due to cooling from the mold wall. Given that such a front is seldom observed in conventional alloy castings, it is not likely to be observed here.

6. *Boundary 3-4*

This boundary is the infiltration front in cases where the initial fiber preform temperature is sufficiently high not to cause solidification of the metal. Region 1 will still be present if there is significant cooling at the mold wall and will separate regions 2 and 3.

$$P_3 = P_g + \Delta P_\gamma \quad [29]$$

$$T_3 = T_4 \quad [30]$$

$$(\mathbf{k}_p \nabla T_4) \cdot \mathbf{n}_{3,4} = (\mathbf{k}_c \nabla T_3) \cdot \mathbf{n}_{3,4} \quad [31]$$

$$\mathbf{v}_{o1} = (1 - V_f)\mathbf{v}_{3,4} \quad [32]$$

7. *Boundary 5-4*

This is the infiltration front when the initial fiber temperature is low enough to cause eutectic solid to form. Equations are analogous to those for infiltration with a pure metal into a sufficiently cold preform (Eqs. [14] through [17] of Reference 1).

$$P_5 = P_g + \Delta P_\gamma \quad [33]$$

$$T_4 = T_5 = T_E \quad [34]$$

$$(\mathbf{k}_p \nabla T_4) \cdot \mathbf{n}_{4,5} = (1 - V_f) g_{sE} \Delta H \rho_m \mathbf{v}_{4,5} \quad [35]$$

$$\mathbf{v}_{o5} = (1 - V_f)\mathbf{v}_{5,4} \quad [36]$$

where g_{sE} is the fraction solid in region 5.

With specification of system constants and functions of the process geometry and of its parameters, the problem is specified. Expressions for preform permeability (with no solid metal present) and composite thermal conductivity are identical to those given in Section III–D of Reference 1.

IV. UNIDIRECTIONAL ADIABATIC INFILTRATION UNDER CONSTANT APPLIED PRESSURE

A. *Description*

We now focus attention on the case of unidirectional adiabatic infiltration, along the x-axis, of a semi-infinite fiber preform. We assume, furthermore, that infiltration is driven by a constant applied pressure $\Delta P_T = P_0 - P_g$, where P_0 is the pressure in the metal at $x = 0$. The preform is assumed to be uniform and incompressible, with a constant fiber diameter and volume fraction. We neglect the gravitational force field, either in comparison to the applied pressure gradient or because infiltration is horizontal. We assume that the x-axis is a principal direction of thermal conductivity and permeability tensors of the preform and, hence, of the composite.

Since there is no cooling at the mold wall, region 2 does not exist in this case. Figure 2 is a schematic representation of the system in the case where all four regions are present in the composite.

We assume that all the thermal conductivities are independent of temperature in the range considered. We also assume for simplicity that the alloy phase diagram features straight liquidus and solidus lines of respective slopes m_L and m_S and partition ratio k.

Because everywhere in the casting the metal temperature increases with time (the infiltrated composite is cooled at the infiltration front and heated at the gate by incoming metal), the solid phase composition is uniformly equal to

$$C_S = kC_L \quad [37]$$

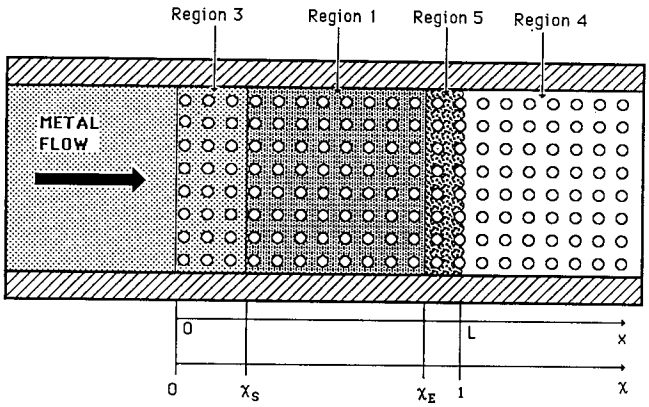

Fig. 2—Schematic illustration of the case of unidirectional adiabatic infiltration with an initial fiber temperature low enough to cause formation of solid eutectic metal. Fiber diameter is exaggerated.

Temperature and liquid composition are linearly related by

$$T - T_m = C_L m_L \qquad [38]$$

where T_m is the melting point of the pure metal.

The governing equations and boundary conditions are the same as for the three-dimensional case, every gradient becoming a simple partial derivative with respect to x.

B. *Transformation of the Equations*

Equations [1] and [2] combine to become

$$(1 - V_f)\frac{dL}{dt} = -\frac{K}{\mu}\frac{dP}{dx} \qquad [39]$$

where L is the position of the infiltration front at time t. With the foregoing assumptions, the permeability K is only a function of local volume fraction solid metal g_s. Let us now "guess" that the infiltration front moves as a constant ψ times the square root of time:

$$L = \psi\sqrt{t} \qquad [40]$$

We define a new variable $\chi = x/\psi\sqrt{t}$ and operate a Boltzmann transformation on the governing equations and all equations at the moving boundaries in order to reduce the two parameters x and t to the single parameter χ. In what follows, we prove that all governing equations, interphase equilibrium equations, and initial and boundary conditions describing the process can be expressed in terms of χ and, hence, that the "similarity" solution procedure we use is valid. This solution is "similar" in that, at any instant, it is identical with a scaling factor $\psi\sqrt{t}$ acting on x.

We define a dimensionless temperature:

$$\Theta = \frac{T - T_m}{m_L C_0} \qquad [41]$$

The set of equations can now be described by the two dimensionless variables Θ and g_s, functions of the single variable χ (temperature, liquid composition, and solid composition are all linearly related (Eqs. [37] and [38]). As depicted in Figure 2, regions 1, 3, 4, and 5 will be found in the order 3, 1, 5, and 4 starting from the preform entrance at $x = 0$. We define χ_s and χ_E as being the dimensionless positions of the boundary between region 1 and regions 3 and 5, respectively, when these boundaries are present. After transformation, the general equations given in Section III take the form below, where prime indicates differentiation with respect to χ. Preceding the equations, we have indicated the original untransformed equation.

In region 1, Eq. [10] ⇒

$$\Theta' = \chi(1 - (1 - k)g_s)\Theta' - \chi\Theta(1 - k)g_s' \qquad [42]$$

and Eq. [3] ⇒

$$\Theta'' = -\alpha\chi\Theta' + \delta\Theta' + \gamma\chi g_s' \qquad [43]$$

where

$$\alpha = \frac{\rho_c c_c \psi^2}{2k_c}$$

$$\delta = \frac{(1 - V_f)\rho_m c_m \psi^2}{2k_c}$$

and

$$\gamma = \frac{(1 - V_f)\rho_m \Delta H \psi^2}{2k_c m_L C_0}$$

In region 3, Eq. [5] ⇒

$$(\chi - \beta)\Theta' = -\frac{2\alpha_c}{\psi^2}\Theta'' \qquad [44]$$

and (by definition)

$$g_s = 0 \qquad [45]$$

where

$$\alpha_c = \frac{k_c}{\rho_c c_c}$$

and

$$\beta = \frac{\rho_m c_m (1 - V_f)}{\rho_c c_c}$$

In region 4, Eq. [6] ⇒

$$\chi\Theta' = -\frac{2\alpha_p}{\psi^2}\Theta'' \qquad [46]$$

where

$$\alpha_p = \frac{k_p}{\rho_p c_p}$$

And in region 5,

$$\Theta = \Theta_E \qquad [47]$$

$$g_s = \text{constant} \qquad [48]$$

where Θ_E is dimensionless eutectic temperature. Equilibria at the interregion boundaries dictate, after transformation:

At $\chi = 0$,

$$\Theta = \Theta_0 \qquad [49]$$

where Θ_0 is dimensionless initial metal temperature.

At $\chi = \chi_s$, Eq. [18] $\Rightarrow$

$$\Theta'_{(\chi_s^+)} - \Theta'_{(\chi_s^-)} = \frac{(1 - V_f)\rho\,\Delta H\,\psi^2 g_s}{2k_c m_L C_0}\,\chi_s \qquad [50]$$

and Eq. [17] $\Rightarrow$

$$\chi_s\{\Theta[1 - (1 - k)g_s] - 1\} = \Theta - 1 \qquad [51]$$

If some eutectic, *i.e.*, region 5, is present, we have:

At $\chi = \chi_E$,

$$\Theta = \Theta_E \qquad [52]$$

Eq. [28] $\Rightarrow$

$$g_s = 0 \qquad [53]$$

and Eq. [27] $\Rightarrow$

$$\Theta'_{(\chi_E^-)} = -\frac{(1 - V_f)\rho\,\Delta H\,\psi^2 g_{sE}}{2k_c m_L C_0}\,\chi_E \qquad [54]$$

And at $\chi = 1$, Eq. [34] $\Rightarrow$

$$\Theta = \Theta_E \qquad [55]$$

and Eq. [35] $\Rightarrow$

$$\Theta'_{(1^+)} = -\frac{(1 - V_f)\rho\,\Delta H\,\psi^2 g_{sE}}{2k_p m_L C_0} \qquad [56]$$

Conversely, if no solid eutectic metal is present but solid primary metal forms during infiltration, we have:

At $\chi = 1$, Eq. [22] $\Rightarrow$

$$g_s = 0 \qquad [57]$$

and Eq. [23] $\Rightarrow$

$$\Theta'_{(1^-)} = \frac{k_p}{k_c}\,\Theta'_{(1^+)} \qquad [58]$$

Finally, since temperature and fraction solid metal are now clearly only functions of χ and since permeability is only a function of fraction solid metal, K is only a function of χ. From Eq. [39], then, pressure P is only a function of χ as well. By integration of Eq. [39] in x, we then find

$$(1 - V_f)L\frac{dL}{dt} = -\int_0^1 \frac{K}{\mu}\frac{dP}{d\chi}\,d\chi \qquad [59]$$

Since the right-hand term is independent of time, our previous guess that $L/\sqrt{t} = \psi$ is a constant is internally consistent.

This treatment of the problem introduces an assumption. Since at $t = 0$, the velocity is infinite and Darcy's law cannot be valid, we must, therefore, assume that after a transient period during which flow is governed by the complete Ergun equation, the solution to our problem converges rapidly to that given by the similarity solution.

C. *Solution of the Equations*

In region 3, the temperature profile is readily given as in Reference 1:

$$\frac{\Theta - \Theta(\chi_s)}{\Theta_0 - \Theta(\chi_s)} = \frac{\operatorname{erf}\left(\frac{\psi}{2\sqrt{\alpha_c}}(\chi - \beta)\right) - \operatorname{erf}\left(\frac{\psi}{2\sqrt{\alpha_c}}(\chi_s - \beta)\right)}{\operatorname{erf}\left(\frac{\psi}{2\sqrt{\alpha_c}}(-\beta)\right) - \operatorname{erf}\left(\frac{\psi}{2\sqrt{\alpha_c}}(\chi_s - \beta)\right)} \qquad [60]$$

In region 4, we obtain, again as in Reference 1,

$$\frac{\Theta - \Theta_f}{\Theta(1) - \Theta_f} = \frac{\operatorname{erfc}\left(\frac{\psi}{2\sqrt{\alpha_p}}\chi\right)}{\operatorname{erfc}\left(\frac{\psi}{2\sqrt{\alpha_p}}\right)} \qquad [61]$$

where Θ_f is dimensionless initial preform temperature.

Analysis of the process when the fiber temperature is sufficiently high for no solid metal to form is analogous to that given in Reference 1. The temperature profile and rate of infiltration are calculated for this case as in Section V–A of that paper. The composition is obviously everywhere equal to the nominal composition of the alloy that is injected at $x = 0$. The range of initial fiber temperatures T_f for which no solid will form is similarly given by satisfaction of inequality [46] of Reference 1, with the alloy liquidus replacing the melting point of the pure metal.

When T_f is too low for inequality [46] of Reference 1 to be satisfied, solid metal will form between the fibers during infiltration. Region 1 and, perhaps, region 5 are then present in the infiltrated composite.

In region 1, the system of equations consists of two nonlinear differential equations, one of second order and the other of first order. A brief mathematical study of this system led us to the conclusion that there is no simple analytical solution. The point $\chi = 0$ is a singular point, where all the derivatives of temperature and fraction solid are equal to zero (Appendix). The system does not otherwise present any odd points, and we can assume that temperature and fraction solid are continuous and differentiable four times in that region. This system is equivalent to a system of three differential equations of the first order in one variable. We then need to consider three functions, namely, Θ, Θ', and g_s. We solve the system numerically, using a Taylor series expansion for Θ, Θ', and g_s up to the third order.[15]

We consider first the case where the entire infiltrated composite belongs to region 1, *i.e.*, where there is no superheat in the metal and an initial fiber temperature that is sufficiently high that no solid eutectic metal forms at the front.

The boundary conditions give the value of g_s and Θ' as a function of Θ at $\chi = 1$, and the value of Θ, which should be 1 (nominal composition), at $\chi = 0$. Given the presence of a singular point at $\chi = 0$, the calculation of temperature and fraction solid metal profiles are done starting from $\chi = 1$. An arbitrary value for dimensionless temperature Θ at $\chi = 1$ is first used, and the functions g_s, Θ, and Θ' are calculated point by point toward

$\chi = 0$ using the Taylor expansion method with a step $h = -0.01$. The value of function F at the point $x + h$ is written as

$$F(x + h) = F(x) + hF'(x) + \frac{h^2}{2}F''(x) + \frac{h^3}{6}F'''(x) + o(h^4)$$

Adjustments are made to the initial guess of Θ at $\chi = 1$ by a test comparing Θ at $\chi = 0$ obtained with the expected value of 1 and varying Θ at $\chi = 1$ using a proportional scheme with an under-relaxation coefficient of 1. This procedure is carried out iteratively until $\Theta = 1 \pm 0.007$ at $\chi = 0$. At this time, global conservation of heat and solute is also verified by integration of the calculated profiles.

As in Reference 1 for pure aluminum, we found no difference in results for δ-alumina fibers infiltrated with Al-4.5 wt pct Cu when taking into account heat transfer ahead of the infiltration front and when neglecting heat transfer into the fiber preform. In the latter case, the boundary condition

$$\Theta'_{(1^-)} = \frac{\rho_p c_p \psi^2}{2k_c}(\Theta_f - \Theta_{(1^-)}) \qquad [62]$$

is used instead of Eq. [58]. This equation can be derived from first principles or alternatively by combining Eqs. [58] and [61] and taking the limit as $\psi/\sqrt{\alpha_p} \to \infty$. Results given below for δ-alumina fibers infiltrated with Al-4.5 wt pct Cu were performed using Eq. [62] instead of Eqs. [58] and [61].

If there is no superheat in the entering metal, but solid eutectic forms at the infiltration front (*i.e.*, region 5 exists), the relevant boundary conditions for region 1 are given by Eqs. [52] through [56]. The volume fraction of solid eutectic metal $g_{s,E}$ in region 5 is given by Eqs. [56] and [61] if there is significant conduction of heat into the preform. These equations can be combined, as with a pure metal, to yield the following expression when the preform thermal conductivity is sufficiently low:

$$g_{s,E} = \frac{\rho_f c_f V_f (T_E - T_f)}{\rho_m \Delta H (1 - V_f)} \qquad [63]$$

In this case, the procedure used to derive temperature and fraction solid metal within the infiltrated composite is similar to that used with no eutectic, except that the variable parameter for the iteration is Θ at $\chi = \chi_E$ (instead of Θ at $\chi = 1$ with no eutectic). In a similar fashion, adjustments are made to the guessed value of χ_E by comparing Θ at $\chi = 0$ obtained with the expected value of 1.

When the incoming metal is superheated, region 3 is present. The additional boundary conditions are given by Eqs. [49] through [51]. Between $\chi = 0$ and $\chi = \chi_s$, the solution is given by Eqs. [46] and [60]. With no eutectic at the infiltration front, an arbitrary Θ at $\chi = 1$ is chosen, and Θ and g_s are calculated as before using Taylor series. From Eq. [51] and the Θ and g_s profiles, χ_s is calculated. From Eqs. [50] and [60] and the resulting value for χ_s, another value of g_s is calculated and compared to that obtained previously *via* the Taylor series solution. The final solution is obtained by iteration, varying the value of Θ at $\chi = 1$, and using a proportional scheme based on a comparison of the two values of g_s calculated as described above.

Because, as will be seen in Section V, region 5 is seldom observed with δ-alumina fibers infiltrated with Al-4.5 wt pct Cu, the case of eutectic forming with superheated metal at the gate was not investigated.

D. *Limiting Case of Negligible Thermal Conduction*

Derivation of the solute and temperature profiles is particularly simple in the limiting case of negligible thermal conduction in the composite when $\psi/\sqrt{\alpha_c} \to \infty$ (using data in Figure 4 of Reference 1, $\psi/\sqrt{\alpha_c} > 10$ should suffice). In this case, inspection of Eq. [43] indicates that $\Theta' \to 0$ and, therefore, from Eq. [42], $g'_s \to 0$. Thus, temperature and fraction solid are constant in region 1.

When $T_E < T_f < T_L$, where T_L is the metal liquidus and T_E is the eutectic temperature, solid primary metal forms. Because of solute rejection and because g_s cannot be finite at the infiltration front, there is a zone of liquid metal preceding region 1 at the infiltration front. Temperature, composition, and fraction solid profiles along the composite thus take the form depicted schematically in Figure 3(a). The temperature in the liquid zone preceding region 1 is necessarily the initial fiber temperature T_f. The metal composition in this liquid zone is that of the liquidus at T_f, $C_{L,f}$, because a higher solute content could only result from a temperature excursion below T_f, which would have no physical justification. Derivation of the five unknowns χ_s, χ_L (position of the boundary between region 1 and the fully liquid zone at the infiltration front), T_1 (temperature in region 1), $C_{L,1}$ (liquid composition in region 1), and g_s (fraction solid in region 1) results, in a simple manner, from Eq. [38] and conservation equations at $\chi = \chi_s$ and χ_L:

Heat conservation at $\chi = \chi_s$:

$$(1 - V_f)\rho_m c_m (T_0 - T_1) = \chi_s[\rho_c c_c (T_0 - T_1) - g_s \rho_m \Delta H (1 - V_f)] \qquad [64]$$

Solute conservation at $\chi = \chi_s$:

$$C_0 - C_1 = \chi_s[C_0 - (1 - (1 - k)g_s)C_{L,1}] \qquad [65]$$

Heat conservation at $\chi = \chi_L$:

$$(1 - V_f)\rho_m c_m (T_1 - T_f) = \chi_L[\rho_c c_c (T_1 - T_f) + g_s \rho_m \Delta H (1 - V_f)] \qquad [66]$$

Solute conservation at $\chi = \chi_L$:

$$C_{L,f} - C_1 = \chi_L[C_{L,f} - (1 - (1 - k)g_s)C_{L,1}] \qquad [67]$$

Global conservation of heat and solute in the composite is verified by addition of Eqs. [64] and [66] and subtraction of Eq. [67] from Eq. [65], respectively.

In the event where $T_f < T_E$, eutectic metal forms at the infiltration front. A zone of solid and liquid eutectic metal then replaces the liquid zone ahead of region 1. Fraction solid, temperature, and liquid composition profiles are now as depicted in Figure 3(b). The fraction

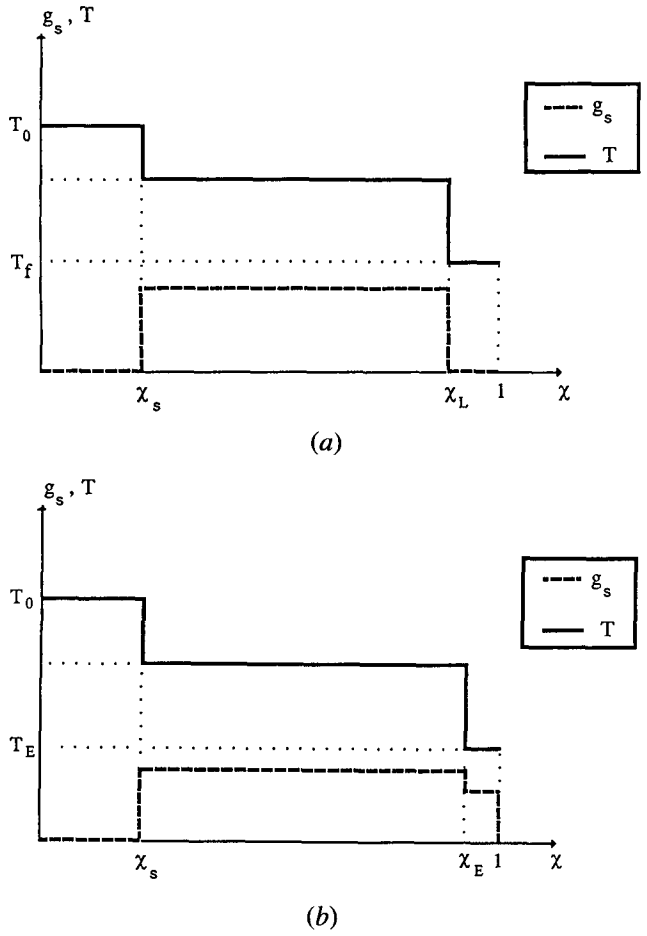

Fig. 3—Temperature and fraction solid profiles for unidirectional adiabatic infiltration with negligible thermal conduction in the composite, (*a*) with an initial fiber temperature low enough to cause formation of primary solid but not eutectic solid metal and (*b*) with an initial fiber temperature low enough to cause formation of solid eutectic metal at the infiltration front.

eutectic is given by Eq. [63]. The five unknowns $g_{s,1}$ (fraction solid metal in region 1), χ_s, χ_E, T_1, and $C_{L,1}$ result in a similar manner from Eqs. [38], [64], and [65] and conservation equations at $\chi = \chi_E$.

Heat conservation at $\chi = \chi_E$ dictates

$$(1 - V_f)\rho_m c_m (T_1 - T_E) = \chi_E[\rho_c c_c (T_1 - T_E) + (g_{s,1} - g_{s,E})\rho_m \Delta H (1 - V_f)] \quad [68]$$

while solute conservation at $\chi = \chi_L$ yields

$$C_E - C_1 = \chi_E[C_E - (1 - (1 - k)g_{s,1})C_{L,1}] \quad [69]$$

The limiting case of infinitely fast conduction, *i.e.*, $\psi\sqrt{\alpha_c} \to 0$ and, in practice, smaller than at most 0.1, is of no particular interest since no solid metal will form and the temperature will be uniformly at T_0 in the composite (Eqs. [43] and [46] and Figure 4, all in Reference 1).

V. RESULTS FOR δ-ALUMINA FIBERS INFILTRATED WITH Al-4.5 WT PCT Cu

Using the approach described in Section IV–C, temperature, volume fraction solid, and composition were calculated for infiltration of 24 vol pct δ-alumina fibers with Al-4.5 wt pct Cu. Numerical values adopted for heat capacities, heat of fusion, thermal conductivities, viscosity, and densities are the same as those used for infiltration with pure Al given in Table II of Reference 7. The phase diagram features liquidus and solidus boundaries that are almost linear, with $m_L = -3.36$ K/wt pct Cu and $k = 0.171$.[16]

Plots of temperature, volume fraction solid, and average metal matrix composition along the length of the composite are given in Figures 4 and 5 for two cases of

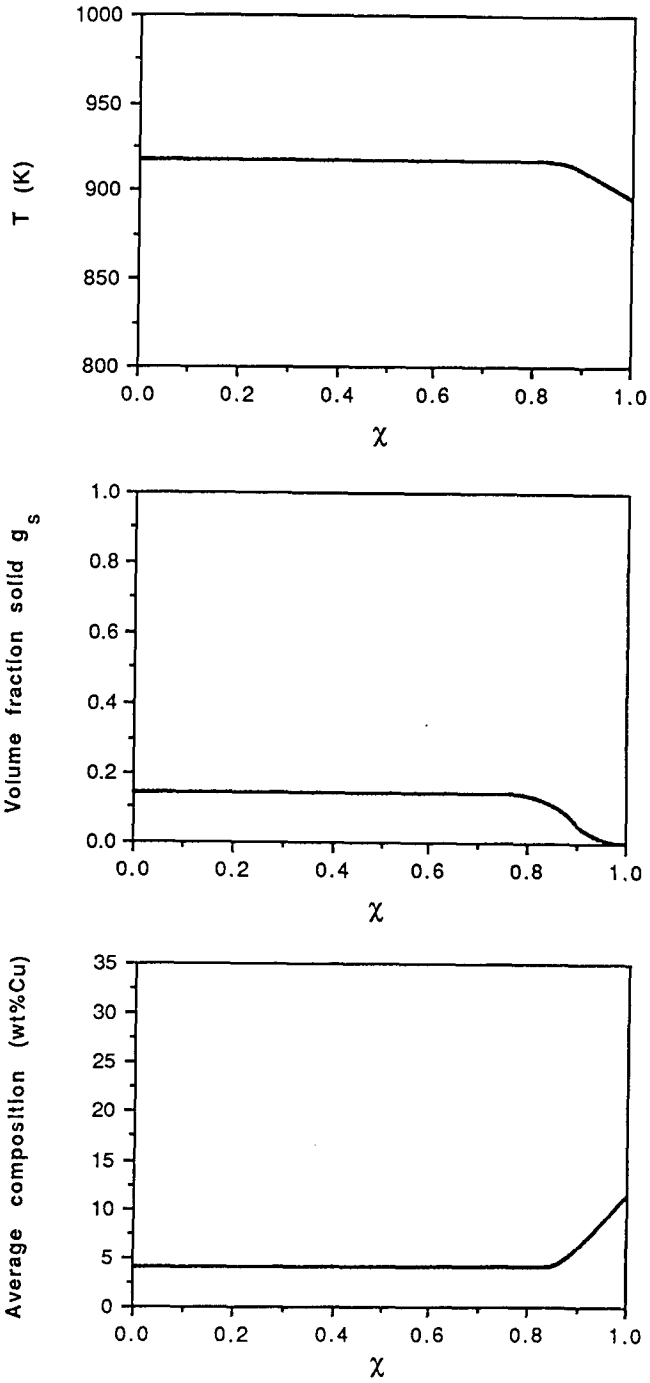

Fig. 4—Temperature, fraction solid, and average matrix composition along the infiltrated composite during adiabatic unidirectional infiltration under constant applied pressure of 24 vol pct δ-alumina preforms with Al-4.5 wt pct Cu. $T_f = 823$ K and $\psi = 0.018$ m/$\sqrt{s}$, with no superheat.

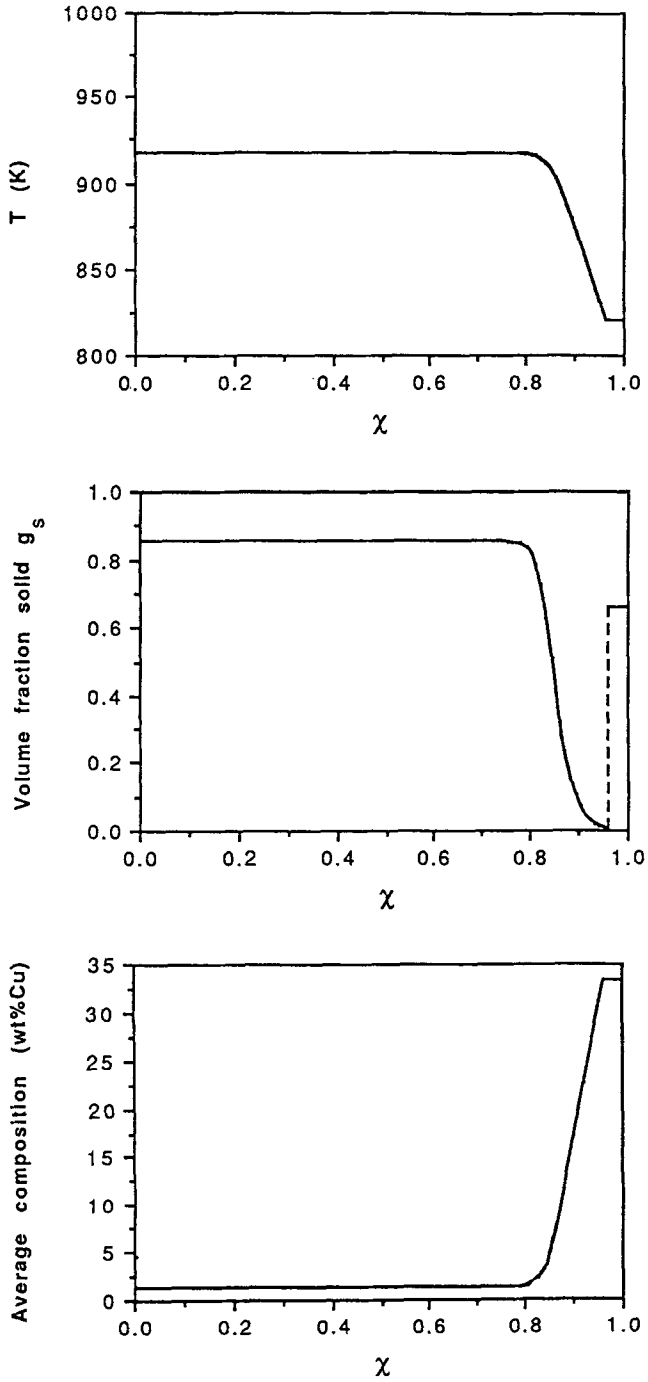

Fig. 5—Temperature, fraction solid, and average matrix composition along the infiltrated composite during adiabatic unidirectional infiltration under constant applied pressure of 24 vol pct δ-alumina preforms with Al-4.5 wt pct Cu. T_f = 323 K and ψ = 0.015 m/$\sqrt{s}$, with no superheat.

no metal superheat without and with the formation of solid eutectic, respectively. Each of these variables is constant over most of the sample length. Most of the matrix is, therefore, of uniform composition, albeit lower than the nominal 4.5 wt pct Cu. This happens because a steep temperature gradient is needed at the infiltration front to heat the fibers (unlike the case of infiltration by a pure metal, matrix solidification can only heat the fibers from behind the infiltration front *via* conduction through the composite lying upstream). Matrix solidification, therefore, takes place over a relatively short distance behind the infiltration front.

Conditions of ψ and T_f needed for solid eutectic to form with no superheat are given in Figure 6. Very low T_f, far below T_E (821 K), can be used while still avoiding formation of solid eutectic at the infiltration front. Eutectic formation is prevented by conduction of heat through the composite to the infiltration front. Therefore, the higher the infiltration rate (measured by ψ), the higher the preform temperature below which heat conduction cannot keep up with cooling by the fibers causing solid eutectic to form.

With superheated metal, region 3 appears. This results in a zone of matrix composition C_0 extending from $\chi = 0$. Temperature, fraction solid, and composition profiles are given in Figures 7 and 8 for two sets of infiltration parameters. It is seen that relatively small and physically plausible variation of these parameters results in very different profiles of temperature, fraction solid, and average composition. Conditions in Figure 8 lead to unfavorable infiltration kinetics compared to conditions in Figure 7, because there is a sharp maximum in fraction solid around $\chi = 0.5$ and, hence, a "bottleneck" of low permeability at that point.

Even small superheat results in a large remelted region within the composite (Figure 9). This is significant because the presence of this remelted region results in macrosegregation and microstructural heterogeneity within the composite.[9] Casting with low T_f is generally motivated by the desire to avoid extensive fiber/matrix reactions, a purpose which is defeated within region 3 of the composite. Furthermore, superheat lowers the minimum composition observed in the composite (Figure 10). For these reasons, superheat in the metal should be kept as small as possible when casting composites with a low fiber temperature.

Decreasing T_f decreases the minimum composition observed in the composite, as seen in Figure 11 for two different values of T_0. The minimum matrix solute content decreases as T_f decreases, but the liquid composition and, hence, the temperature at this point are hardly affected. Therefore, it is mostly through an increase in

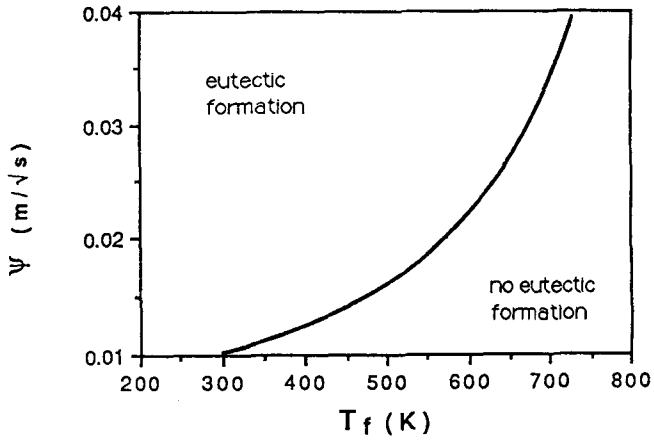

Fig. 6—Conditions for formation of solid eutectic metal during adiabatic unidirectional infiltration under constant applied pressure of 24 vol pct δ-alumina preforms with Al-4.5 wt pct Cu and with no superheat in the metal.

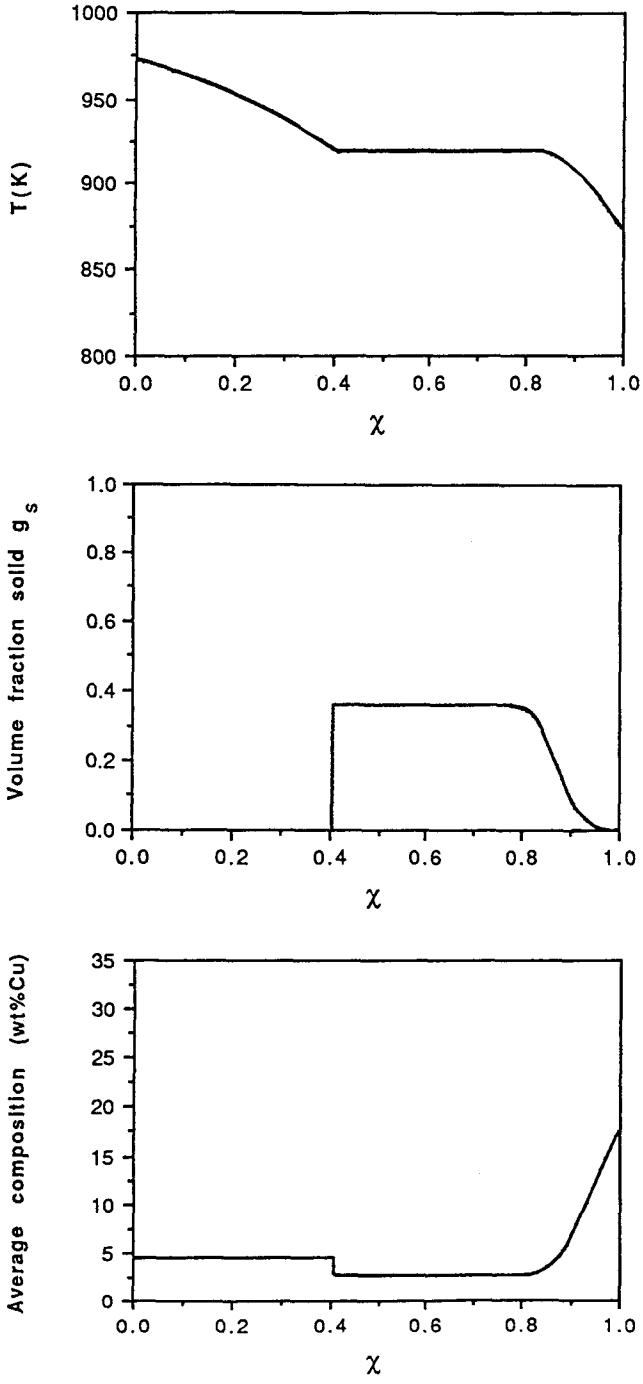

Fig. 7—Temperature, fraction solid, and average matrix composition along the infiltrated composite during adiabatic unidirectional infiltration under constant applied pressure of 24 vol pct δ-alumina preforms with Al-4.5 wt pct Cu. T_f = 673 K, ψ = 0.015 m/$\sqrt{s}$, and T_0 = 973 K.

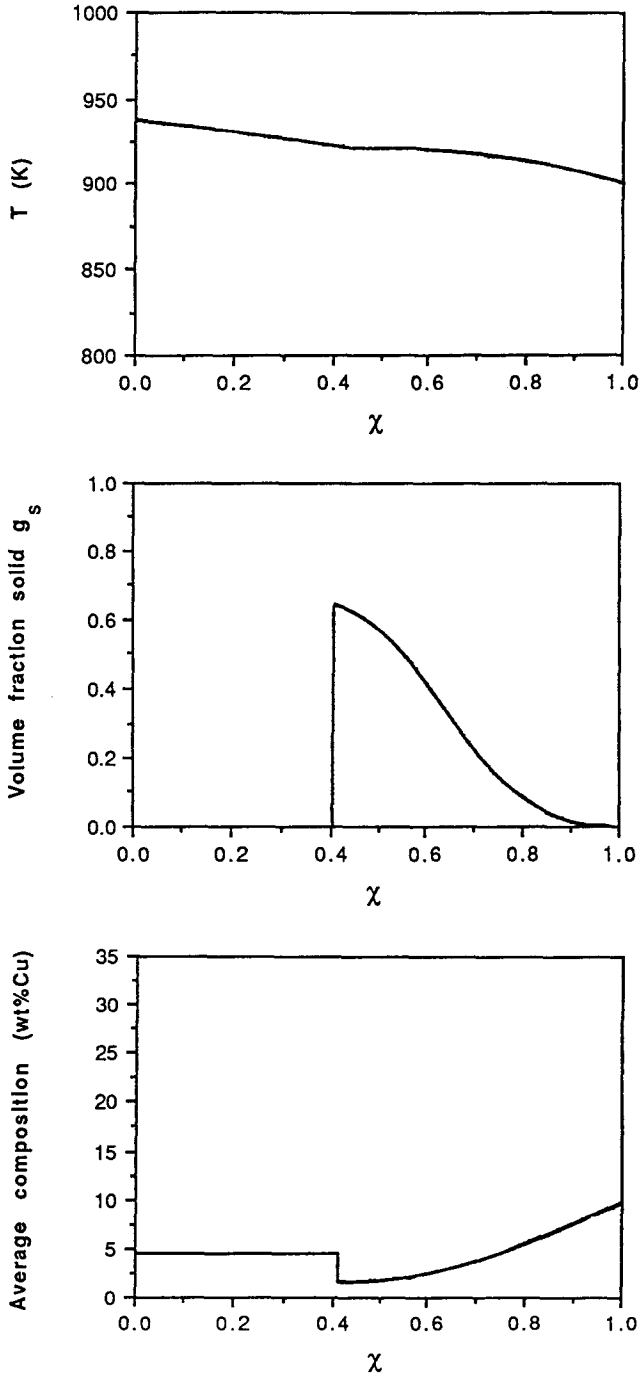

Fig. 8—Temperature, fraction solid, and average matrix composition along the infiltrated composite during adiabatic unidirectional infiltration under constant applied pressure of 24 vol pct δ-alumina preforms with Al-4.5 wt pct Cu. T_f = 571 K, ψ = 0.005 m/$\sqrt{s}$, and T_0 = 938 K.

fraction solid metal that the matrix composition varies. This result is obvious with no superheat in the metal (Figure 11(a)) but not when superheat is present (Figure 11(b)). The influence of T_f on the maximum matrix solute content which is found at the infiltration front is given in Figure 12 for the same values of T_0 used in Figure 11. In both cases, the lower the preform temperature, the higher the degree of solute enrichment at the infiltration front.

Infiltration kinetics, measured by ψ, also strongly affect solute enrichment at the infiltration front (Figure 13). As ψ increases, the temperature at the infiltration front decreases because the fibers at the infiltration front are heated less by conduction; accordingly, there is a corresponding increase in the copper concentration.

The initial fiber temperature T_f should be kept sufficiently high to satisfy inequality [46] of Reference 1 (with liquidus temperature replacing melting point) to avoid macrosegregation and microstructural heterogeneity in the composite. However, if it is desired to effect

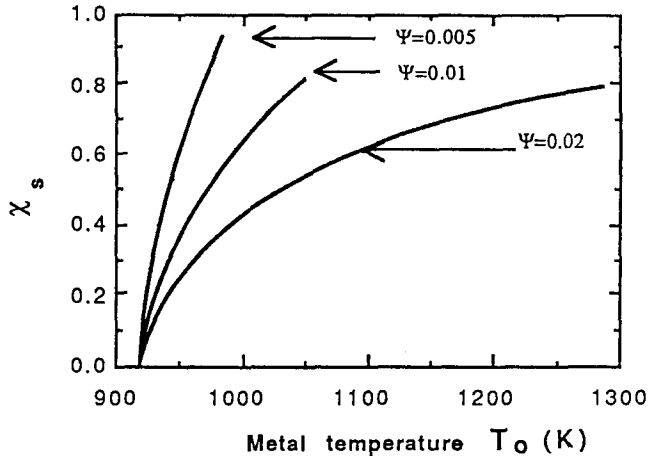

Fig. 9—Position of the remelting front χ_s during adiabatic unidirectional infiltration under constant applied pressure of 24 vol pct δ-alumina preforms with Al-4.5 wt pct Cu with an initial fiber temperature T_f = 673 K as a function of superheat and for three infiltration velocities ψ, given in m/√s.

matrix solidification during infiltration (to minimize fiber/matrix reactions or to control matrix microstructure), then the resulting macrosegregation is strongly dictated by the choice of processing variables, T_f, T_0, and ψ. Superheat in the metal should be avoided for reasons given above. With this proviso, T_f and ψ (in practice, T_f and applied pressure P_0) can be selected so that most of the casting is of uniform structure and composition. Figures 14 and 15 give the values of χ, χ_{99}, below which the relative variation in matrix composition is less than 1 pct in a sample cast with no superheat. The value χ_{99} is defined by

$$\frac{\bar{C}(\chi_{99}) - \bar{C}(0)}{\bar{C}(0)} = 0.01 \qquad [70]$$

When the initial fiber preform temperature is more than 50 K below the liquidus temperature of the metal, there is practically no dependence of χ_{99} on T_f. Conversely, the dependence of χ_{99} on ψ is strong (Figure 15). These curves indicate two possible strategies for casting a composite of high compositional homogeneity over a significant fraction of its length: (1) raise T_f to a value very

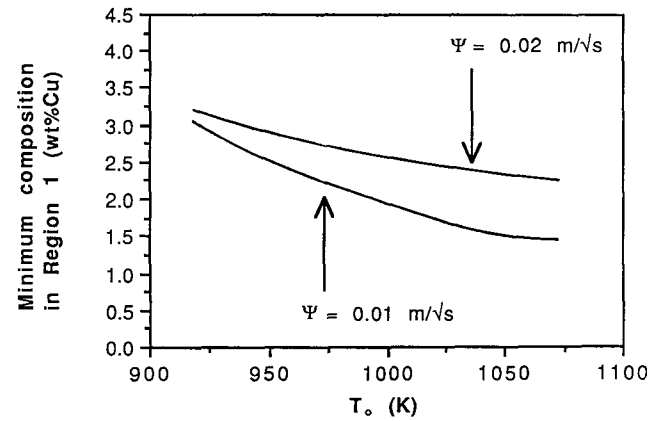

Fig. 10—Minimum average matrix composition in region 1 (at $\chi = \chi_s$) during adiabatic unidirectional infiltration under constant applied pressure of 24 vol pct δ-alumina preforms with Al-4.5 wt pct Cu with an initial fiber temperature T_f = 673 K as a function of superheat for ψ = 0.01 m/√s and ψ = 0.02 m/√s.

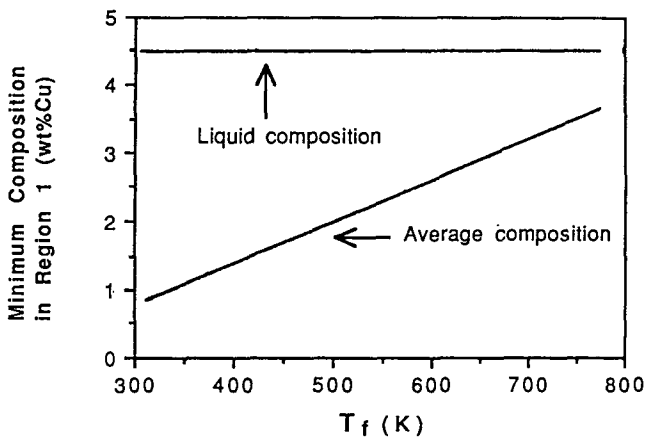

(a)

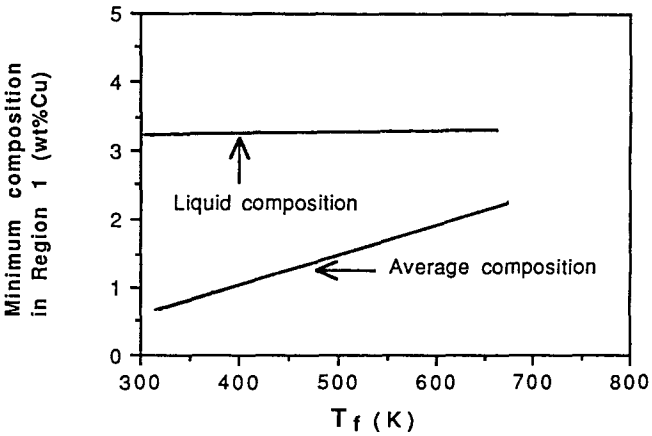

(b)

Fig. 11—Minimum average and liquid matrix composition in region 1 (at $\chi = \chi_s$) during adiabatic unidirectional infiltration under constant applied pressure of 24 vol pct δ-alumina preforms with Al-4.5 wt pct Cu as a function of initial fiber temperature T_f with ψ = 0.01 m/√s for (*a*) no superheat and (*b*) T_0 = 973 K.

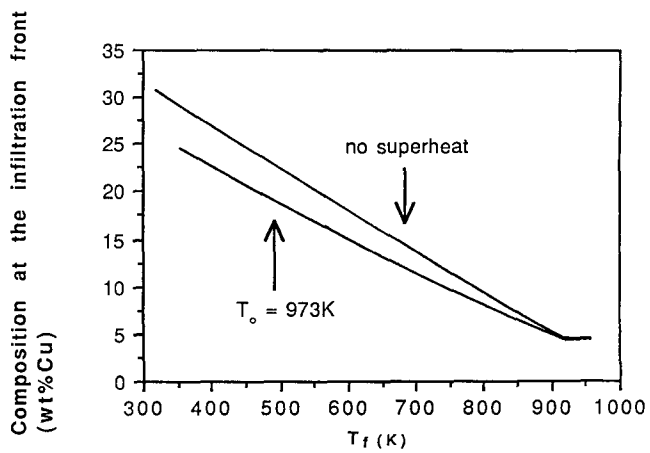

Fig. 12—Composition at the infiltration front (the point of maximum copper concentration in the composite) during adiabatic unidirectional infiltration under constant applied pressure of 24 vol pct δ-alumina preforms with Al-4.5 wt pct Cu as a function of initial fiber temperature T_f with ψ = 0.01 m/√s for (a) no superheat and (b) T_0 = 973 K.

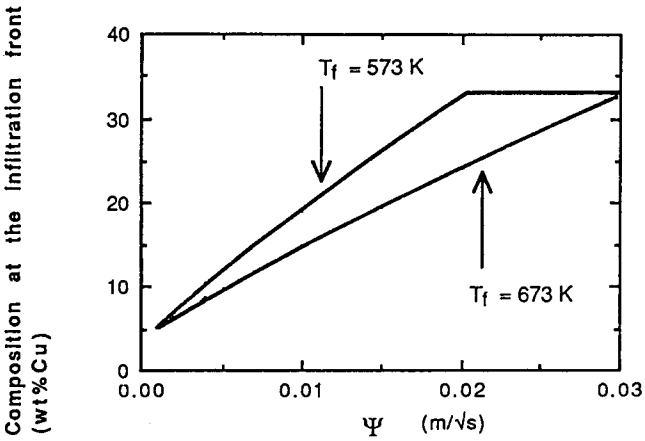

Fig. 13—Composition at the infiltration front (the point of maximum copper concentration in the composite) during adiabatic unidirectional infiltration under constant applied pressure of 24 vol pct δ-alumina preforms with Al-4.5 wt pct Cu as a function of ψ with no superheat.

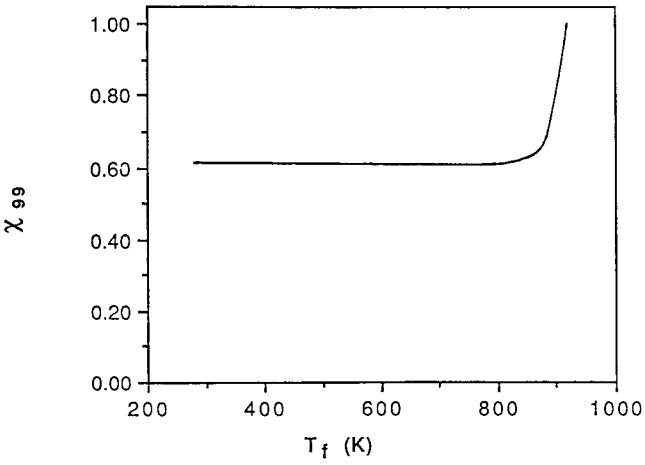

Fig. 14—The value χ_{99}, defined by Eq. [70], during adiabatic unidirectional infiltration under constant applied pressure of 24 vol pct δ-alumina preforms with Al-4.5 wt pct Cu as a function of T_f for $\psi = 0.01$ m/$\sqrt{s}$ and no superheat in the metal.

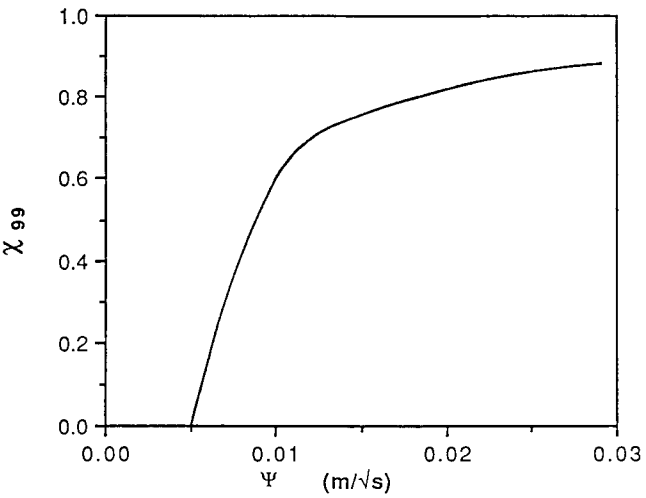

Fig. 15—The value χ_{99}, defined by Eq. [70], during adiabatic unidirectional infiltration under constant applied pressure of 24 vol pct δ-alumina preforms with Al-4.5 wt pct Cu as a function of ψ for both T_f = 573 and 673 K (curves coincide) and no superheat in the metal.

close to the alloy liquidus or (2) increase infiltration velocity. Following this latter strategy, macrosegregation can be suppressed in more than 80 pct of the Al-4.5 wt pct Cu matrix alumina-reinforced composites if $\psi > 0.02$ m/$\sqrt{s}$ for a wide range of initial fiber preform temperatures (Figure 15). If a completely homogeneous composite is desired, the composition transient at the infiltration front can be eliminated by the use of a reservoir at the end of the preform into which solute-rich liquid is evacuated after infiltration of the preform is complete.

The results in Figures 13 and 15 also indicate that ψ must at least be higher than 0.03 m/$\sqrt{s}$ for thermal conduction to be neglected. This corresponds to $\psi/\sqrt{\alpha_c} = 6.5$ which reinforces the statement made earlier that the simplified solution presented in Section IV–D should only be used when $\psi/\sqrt{\alpha_c} > 10$. Such could be the case when infiltrating relatively large fibers using a process such as squeeze casting where applied pressure is very high (on the order of 100 MPa). However, Darcy's law may not be valid in this case (Appendix I in Reference 1).

Comparison of the present theory with experimental data will be published in a later paper.

VI. CONCLUSIONS

General expressions are given to model heat, mass, and fluid flow during infiltration with a hypoeutectic alloy. These and analysis of the physics of the problem lead to the following conclusions.

1. Solid metal may form in the composite during infiltration due to chilling by an initially cold preform. This solid metal grows gradually after passage of the infiltration front, while the local temperature increases.
2. Where solid and liquid metal coexist in the composite during infiltration, temperature and composition may vary. Macrosegregation and microstructural heterogeneity are then observed within the composite.
3. In the case of unidirectional adiabatic infiltration driven by a constant applied pressure, a similarity method can be used to reduce the mathematical complexity of the problem. Temperature, composition, and fraction solid within the composite during infiltration can then be calculated using a numerical procedure to solve the equations. When conduction of heat within the composite can be neglected, an analytical solution is obtained. This, however, requires that $\psi/\sqrt{\alpha_c}$ be in excess of at least 10.

Results from calculations on unidirectional adiabatic infiltration under constant applied pressure of 24 vol pct δ-alumina preforms with Al-4.5 wt pct Cu point to several conclusions of engineering interest.

1. Significant macrosegregation results in the composite when solid metal forms during infiltration.
2. When solid metal forms during infiltration, superheat in the melt results in the formation of a zone of remelted metal extending over a significant portion of the composite. This zone causes compositional and microstructural heterogeneity within the composite; therefore, superheat should be avoided.
3. When the initial fiber temperature is sufficiently low, a region within the casting may result where solid and liquid eutectic metal coexist. In the case of 24 vol

pct δ-alumina preforms with Al-4.5 wt pct Cu, very low initial fiber temperatures or very high infiltration rates are required, and this zone is not observed under practical conditions.

4. With an appropriate selection of processing parameters, the composition and microstructure of the composite can be rendered constant over most of its length, even if solid metal forms during infiltration.

APPENDIX

Proof that all derivatives of Θ and g_s are zero at $\chi = 0$

Assume that Θ and g_s are differentiable any large number of times at $\chi = 0$. After differentiation n times, Eqs. [42] and [43] yield, at $\chi = 0$,

$$\Theta^{(n+1)} = n\Theta^{(n+1)} - (1 - k)n[g_s\Theta]^{(n+1)} \quad [A1]$$

$$\Theta^{(n+2)} = -n\alpha\Theta^{(n)} + \delta\Theta^{(n+1)} + n\gamma g_s^{(n)} \quad [A2]$$

Therefore, if all derivatives to order n of g_s and Θ' are nil at $\chi = 0$, from Eqs. [A1] and [A2], respectively, $g_s^{(n+1)}$ and $\Theta^{(n+2)}$ are nil as well at $\chi = 0$.

From Eq. [42], Θ' is nil at $\chi = 0$. From Eq. [43], then, g_s' is nil at $\chi = 0$. From Eq. [42] differentiated once, Θ'' is nil at $\chi = 0$.

The statement that all derivatives of Θ and g_s are zero at $\chi = 0$, then, follows by recurrence.

ACKNOWLEDGMENTS

This work was sponsored by the Innovative Science and Technology Division of the Strategic Defense Initiative Office through the Office of Naval Research, Contract No. N00014-85-K-0645, under the supervision of Dr. S.G. Fishman of ONR and Dr. J.A. Cornie of MIT. Discussions with Professor Merton C. Flemings of MIT are gratefully acknowledged.

REFERENCES

1. A. Mortensen, L.J. Masur, J.A. Cornie, and M.C. Flemings: *Metall. Trans. A*, 1989, vol. 20A, pp. 2535-47.
2. S. Nagata and K. Matsuda: *IMONO*, 1981, vol. 53, pp. 300-04.
3. S. Nagata and K. Matsuda: *Trans. Jpn. Foundrymen's Soc.*, 1983, vol. 2, pp. 616-20.
4. H. Fukunaga: in *Cast Reinforced Metal Composites*, Proc. Conf., Chicago, IL, 1988, S.G. Fishman and A.K. Dhingra, eds., ASM INTERNATIONAL, Metals Park, OH, 1988, pp. 101-07.
5. H. Fukunaga and K. Goda: *J. Jpn. Inst. Met.*, 1985, vol. 49, pp. 78-83.
6. H. Fukunaga and K. Goda: *Bull. JSME*, 1984, vol. 27, pp. 1245-50.
7. L.J. Masur, A. Mortensen, J.A. Cornie, and M.C. Flemings: *Metall. Trans. A*, 1989, vol. 20A, pp. 2549-57.
8. Experimental work by L.J. Masur, cited by J.A. Cornie, A. Mortensen, and M.C. Flemings: *Proc. 6th Int. Conf. on Composite Materials (ICCM 6)*, F.L. Matthews, N.C.R. Buskell, J.M. Hodgkinson, and J. Morton, eds., Elsevier, London, 1987, pp. 2.297-2.319.
9. T.W. Clyne and J.F. Mason: *Metall. Trans. A*, 1987, vol. 18A, pp. 1519-30.
10. M.C. Flemings: *Solidification Processing*, McGraw-Hill, Inc., New York, NY, 1974, pp. 219-24.
11. L.J. Masur, A. Mortensen, J.A. Cornie, and M.C. Flemings: *Proc. 6th Int. Conf. on Composite Materials (ICCM 6)*, F.L. Matthews, N.C.R. Buskell, J.M. Hodgkinson, and J. Morton, eds., Elsevier, London, 1987, pp. 2.320-2.329.
12. A. Mortensen, J.A. Cornie, and M.C. Flemings: *Metall. Trans. A*, 1988, vol. 19A, pp. 709-21.
13. M.C. Flemings: *Solidification Processing*, McGraw-Hill, Inc., New York, NY, 1974, pp. 142-43.
14. M.C. Flemings and G.E. Nereo: *Trans. TMS-AIME*, 1967, vol. 239, pp. 1449-61.
15. F.B. Hildebrand: *Advanced Calculus for Applications*, 1st ed., Prentice-Hall, Englewood Cliffs, NJ, 1962, p. 94.
16. *Metals Handbook*, 8th ed., ASM, Metals Park, OH, 1973, vol. 8, p. 259.